Integration of Resonant and Non-Resonant Antennas for Coverage of 4G LTE Bands in Handheld Terminals

Aykut Cihangir [(1)], Fabien Ferrero [(2)], Gilles Jacquemod [(1)], Patrice Brachat [(3)], Cyril Luxey [(1)]
[(1)] Laboratory EpOC, University of Nice Sophia Antipolis, FRANCE
(Email: acihangir@unice.fr)
[(2)] LEAT-CREMANT-CNRS, FRANCE
(Email: fabien.ferrero@unice.fr)
[(3)] Orange Labs, La Turbie, FRANCE
(Email: patrice.brachat@orange.com)

***Abstract*— A novel approach for antenna designs covering the LTE frequency bands in a mobile handheld terminal is proposed. The concept consists of a low-band antenna operating in the 700-960MHz band, associated with a high-band antenna operating from 1700 to 2700MHz. The two antennas are separately fed and exhibit high port-to-port isolation. The low-band antenna is of "coupling element" type, modified to be hollowed. The space made available inside this hollow coupling element is then used to insert another antenna operating in the higher frequency bands. The port-to-port isolation between the two antenna feeds is increased using both some antenna placement techniques and bandstop behaviors of matching networks in the frequency bands of interest. Two antenna prototypes are designed, manufactured and measured to validate the simulation results. The effect of the user is also investigated via S-parameter and total efficiency measurements.**

***Index Terms*— Handset antennas, Antenna efficiency, Antenna input impedance, LTE frequency bands, User effect.**

I. INTRODUCTION

The functionalities expected from handheld terminals have been subject to a sustained increase during the past decade. The handheld terminals are no longer only a means of wireless voice communication but are also used for data transfer, video calls and web browsing. From the antenna designer's perspective, these newly added functionalities mean higher data transfer rates, which in turns requires covering more frequency bands with reasonable matching and total efficiency. During the past years, the space allocated for the antenna has generally remained unchanged, despite the need of larger operating bandwidths. With the recent introduction of smartphones on the market, this situation was more or less preserved because the total handheld terminal dimensions started to increase (longer and wider printed circuit board).

Today, a generic handheld terminal antenna should be able to cover:

- 700-787MHz (LTE Bands 12-13-17)
- 824-894MHz (US Cellular, Band 5)
- 880-960MHz (GSM900, Band 8)
- 1.71-1.88GHz (DCS1800, Band 3)
- 1.85-1.99GHz (PCS1900, Band 2)
- 1.92-2.17GHz (IMT2100, Band 1)
- 1.71-2.17GHz (AWS, bands 4-10)
- 2.4-2.5GHz (WLAN2400, 802.11b/g/n)
- 2.5-2.69GHz (TDD LTE, Band 41 and FDD LTE, Band 7)

which can be grouped into the following dual-broadband coverage: 700-960MHz and 1.7-2.7GHz [1].

Concerning the typical space allocated for the antenna versus the operating wavelength, the antenna behaves as an electrically-small radiator in the low frequency band, which makes it difficult to function as a wideband antenna (typically 30% bandwidth) with reasonable impedance matching and acceptable total efficiency. Also, as stated in [2-4], the printed circuit board (PCB) ground plane plays a major role as a radiator, especially in the lower-frequency bands (90% of the total radiation comes from the PCB at 900MHz and 50% at 1800MHz), which is fully supported by the dipole-type vertically-polarized radiation pattern observed at low frequencies regardless of the chosen antenna-type placed at the edge of the PCB.

Considering these facts, two types of antennas have generally been proposed up to now, for handheld terminal antennas covering 700-960MHz and 1.7-2.7GHz. The first one is the coupling element (CE), which is a non-resonant type antenna, specifically designed to excite proper currents (chassis modes) on the PCB ground plane [4-6]. Here, the chassis modes are the resonant modes of the metallic part of

the PCB structure (ground plane) according to its shape. In this antenna-scheme, the currents are induced on the ground plane by capacitive excitation and they are obviously stronger close to the resonance frequencies of the ground plane (which depend on its dimensions). For a 100mm ground plane length, the first chassis wavemode (longitudinal mode) occurs around 1.1GHz if a 10mm distance is set between the coupling element and this ground plane. The feeding mechanism of the coupling element is similar to the one of a monopole, with no inductive contact to the PCB ground plane. In this case, the antenna-structure exhibits a low quality-factor and thus high bandwidth potential (BP) is obtained. The input impedance of the antenna is then tuned to the desired value in the frequency band of interest by using a matching network (MN). The main drawback of this approach is the need for a tunable or a complex matching network if dual-band coverage is needed, which increases the losses due to internal resistances of the SMD components. Another disadvantage is the necessity to keep the region between the coupling element and the ground plane clear from any metal components that can distort the E-field distribution in this area and thus reduce the Bandwidth Potential. Some coupling element designs targeting only the GSM/DCS/PCS/UMTS bands with relatively complicated matching networks (two MN branches connected together) have been already presented in [7-8]. In [9], two coupling elements that are separately fed have been used for dual-band operation. A tunable Matching Network topology for a coupling element has been proposed in [10] to cover DVB-H, GSM and UMTS frequency bands. In [11-12], two designs have been proposed to additionally cover the low LTE frequency band starting from 700MHz with still a relatively complex matching network at the coupling element feed.

The second type of antennas, generally proposed for handheld terminals covering 700-960MHz and 1.7-2.7GHz is a parasitic resonator connected to ground, which is capacitively excited by a driven monopole [13-14]. In this type of solution, the higher band coverage is generally obtained by the driven monopole because of a shorter length and the parasitic resonator is responsible for the low frequency-band coverage. The parasitic element is generally resonant at a single frequency in the low band and has a high quality factor; with the currents starting at the driven monopole, circulating along this parasitic and returning back to the monopole feed. This operating mode does not strongly excite the currents on the ground plane. The wideband behavior is therefore achieved by exciting the ground plane currents with the combination of the resonances of the driven monopole and those of the parasitic, and possibly by using a matching network. The main drawback of this approach is generally the complex 3D geometry, which makes the antenna very sensitive to manufacturing tolerances. Another drawback is the relatively low radiation efficiency of the structure around the resonance frequency of the parasitic, owing to the non-proper excitation of the ground plane currents. Some complex 3D antenna designs with meander lines using a grounded parasitic strip for bandwidth enhancement have been already proposed in [15-16]. Similar designs covering also the low LTE band have been presented in [17-22], where a plastic housing for the antenna is taken into account to help decreasing the covered frequency bands down to 700MHz.

In this paper, novel antenna designs for handheld terminals to cover 700-960MHz and 1.7-2.7GHz frequency bands are presented. The new approach consists of using a non-resonant element in combination with a resonant antenna. To operate in the 700-960MHz frequency band (low-band or LB), a non-resonant coupling element is used with an optimized matching network to obtain an "optimally overcoupled" wideband input impedance characteristic. The coupling element we propose is geometrically different from traditional coupling elements that have been proposed to date. In fact, the metal region inside a plain coupling element is removed to form a "hollow coupling element". With this modification, a more space-efficient antenna concept is implemented with no performance trade-off. The additional space, which is now available, is used to integrate a resonant antenna with a separate feed to cover the 1.7-2.7GHz frequency band (high-band or HB).

The port-to-port isolation is maintained at a high level by both placing the high-band antenna in a low electric field region of the structure and by optimizing the matching network of the hollow coupling element to act as a band-stop filter in the high-band. The main advantage of this approach is the very simple antenna geometry (less sensitivity to fabrication tolerances) and the high isolation with a two-feed antenna configuration that obviates the need to use a diplexer within the RF front-end when simultaneously using the low-band and high-band as in inter-band carrier aggregation for LTE.

The second section describes in detail the new "hollow CE" approach with an antenna height of 3mm on an FR4 substrate. This antenna topology is modified in Section III to obtain a fully printed structure on the FR4 substrate. Section IV presents the S-parameter and total efficiency measurements when the hand of the user is taken into account. Finally we include a summary and draw some conclusions in Section V.

II. The Hollow Coupling Element Approach

The proposed approach, which is based on combining a non-resonant CE and a resonant antenna is presented in this section. The LB coverage is achieved with a 3D CE. The HB coverage is then achieved by integrating another antenna with a separate feed.

A. Comparison of the Hollow CE with a Plain CE

As previously mentioned in the introduction, we originally modified the traditional plain CE to obtain a more space-efficient structure with negligible performance trade-off. This approach was recently described by the authors for single band antennas covering only the LB 700-960MHz frequency band [23-24]. The antenna topologies under study can be observed in Fig. 1.

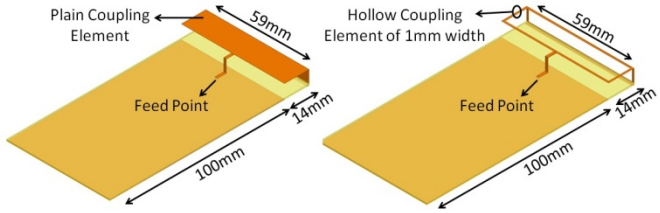

Fig. 1. Antenna topologies used for the plain/hollow CE comparison

The plain CE consists of a rectangular metal sheet ($59\times14mm^2$) located 3mm above the FR4 substrate. The CE is fed through a vertical metal strip from the center of the PCB. The total PCB dimensions are 114×59×0.8mm3 with a ground clearance of 14mm under the CE. For a fair comparison, all the PCB dimensions and feeding location are kept the same for the hollow CE. The metal region inside the plain CE is removed to form the so-called hollow CE, leaving only a rectangular ring having a strip width of 1mm. The two CEs were simulated with the full wave electromagnetic simulator Ansoft HFSS [25]. The simulated input impedance of the two CEs are presented in Fig. 2. The input impedance of the hollow CE shows a minor deviation from the input impedance of the plain CE. The currents induced by the CEs on the system ground plane and the E-field under the CEs at 800MHz are respectively shown in Fig. 3 and Fig. 4. For the hollow CE, it is obvious that the PCB currents are induced in the longitudinal direction of the chassis (fundamental wavemode) as for the plain CE with almost the same strength. The E-field distributions in the vicinity of the ground plane edge are also similar. However, the E-field inside and underneath the hollow CE is weaker than the E-field below the plain CE.

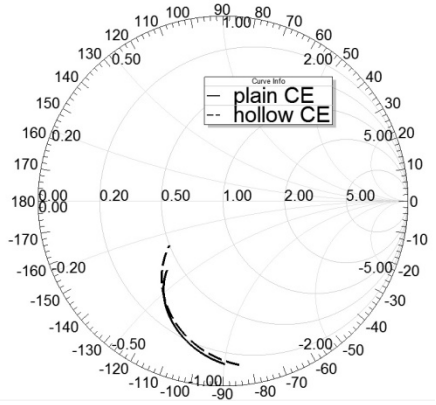

Fig. 2. Input impedance of the plain and the hollow CEs (700MHz to 960MHz)

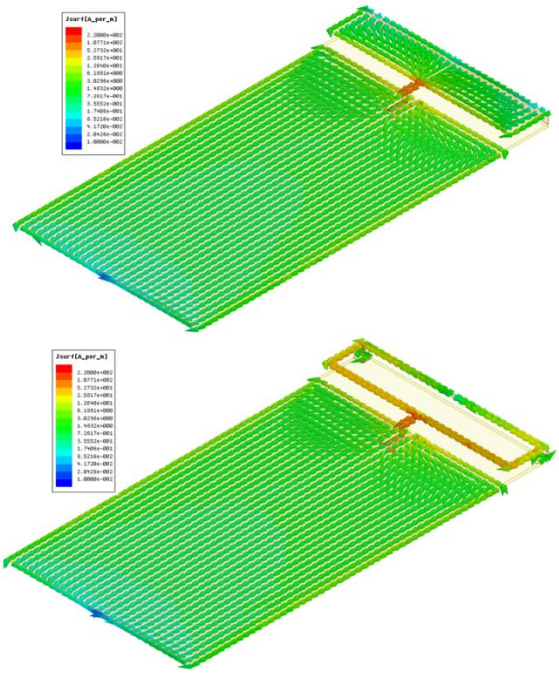

Fig. 3. Comparison of the currents induced on the PCB by the plain CE (top structure) and the hollow CE (bottom structure) at 800MHz

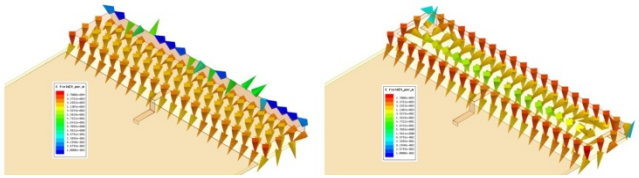

Fig. 4. Comparison of the E-field under the CEs at 800MHz (plain CE on left, hollow CE on right)

The Bandwidth Potential of the two CEs is compared with the help of the commercial software Optenni Lab [26]. The Bandwidth Potential is a realistic value computed from the input impedance of each CE (obtained from the full wave simulation) which is given for a certain number of matching components and a certain threshold for the reflection coefficient. Here, we choose to compute the Bandwidth Potential for a MN composed of only two lumped elements. At every frequency point f_0, the software generates a MN to match as much frequency points as possible around f_0 with a reflection coefficient below the threshold, chosen to be -6dB here. The frequency interval around f_0 which shows a reflection coefficient below -6dB is given as the optimized Bandwidth Potential (symmetrically around f_0). The Bandwidth Potential obtained in this manner is more realistic than the optimistic theoretical values computed from the quality factor. As can be seen in Fig. 5, the Bandwidth Potential of the hollow CE is slightly lower than the Bandwidth Potential of the plain CE, from 650 to 905 MHz, which again proves the equivalence between the plain and the hollow CEs. In the center of the 700-960MHz band, the obtainable Bandwidth Potential is around 200MHz. It should be kept in mind that this Bandwidth Potential value is obtained with a MN of two lumped components which is foreseen to be increased above 260MHz to cover the full LB by using more matching components.

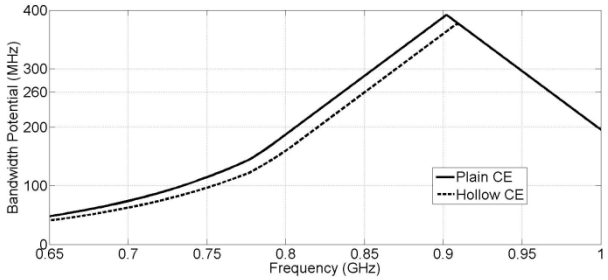

Fig. 5. Bandwidth potential comparison of the two CEs

B. *Integration of High-Band Antenna within the Hollow CE*

As previously mentioned, the space gained by making the plain CE hollow can now be used to integrate a high-band antenna. For ease of manufacturing, we decided to focus on a fully printed HB antenna design (directly on the FR4 substrate). Since we observed that the E-field underneath the hollow CE was weaker in the center of the hollow region (Fig. 4), the HB antenna was placed in this area to obtain high port-to-port isolation. It is observed that a wideband response at HB is required and the broadband behavior cannot be achieved by the HB antenna alone; a beneficial coupling with the LB CE is necessary as will be explained later in the paper.

The optimized layout of the proposed antenna can be seen in Fig. 6. The total PCB dimensions are 114×59×0.8mm^3, with a ground clearance region of 59×14mm^2, reserved for both antennas. The optimized HB antenna is a simple monopole which is placed 8.5mm away from the edge of the PCB. To tune the hollow CE so as to cover the 700-960MHz band, a matching network consisting of four lumped components was designed with the Optenni Lab software (Fig. 7). The primary goal of this optimization was to achieve a reflection coefficient below -6dB between 700-960MHz. Another goal for this MN was to act as a stop-band filter between 1.7-2.7GHz (high reflection coefficient) to help in resisting the possible currents from the HB antenna to reach the LB antenna port. After the circuit optimization of the MN, an additional full-wave optimization was performed to account for the existing transmission lines between the SMD components, the vias connected to the ground plane and the feed point.

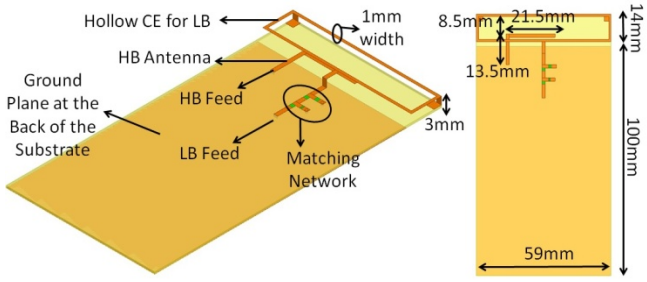

Fig. 6. Optimized layout of the proposed antenna

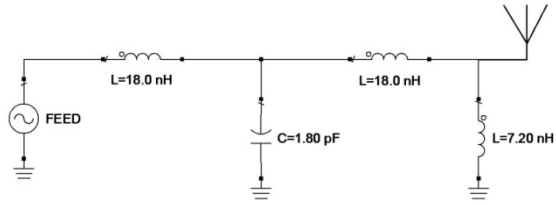

Fig. 7. Optimized matching network used at the LB antenna feed

The simulated input impedance of the LB antenna alone (without the HB antenna) with and without the MN can be seen in Fig. 8 from 700MHz to 960MHz. When the HB antenna is added, the S-parameters seen in Fig. 9 are obtained. The target bands comprising of 700-960MHz and 1.7-2.7GHz are covered with a simulated reflection coefficient below -6dB, except for a small frequency range on the lower edge of the HB (1.7-1.75GHz). The port-to-port isolation is generally higher than 9dB between 700-960MHz with a minimum value of 9.3dB at 740MHz. The port-to-port isolation in the high band is greater than 30dB and therefore it does not appear in Fig. 9 because of the chosen scale.

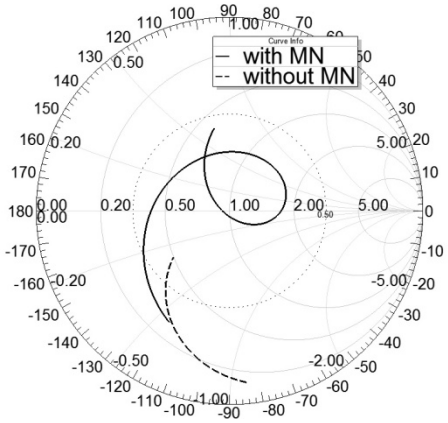

Fig. 8. Input impedance of the LB antenna alone with and without MN from 700 to 960 MHz

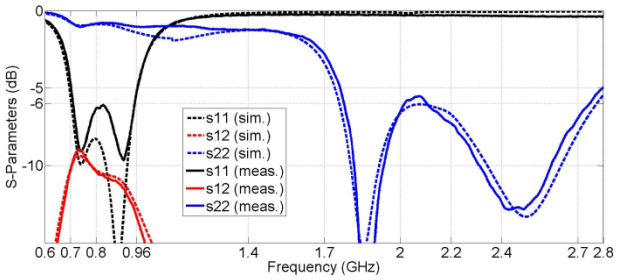

Fig. 9. Simulated and measured S-parameters of the antenna structure presented in Fig. 6

The simulated input impedance of the HB antenna alone and the one of the HB with the LB CE are presented in Fig. 10. It is obvious that the wideband HB response is not due to the HB antenna alone. As may be seen from the Smith Chart plot in Fig. 10, an additional HB resonance is created between 1.7 and 2.7 GHz because of the beneficial coupling with the LB CE's higher order modes. This coupling does not introduce an isolation problem since the MN of the LB antenna is designed on purpose to provide a stop-band

behavior from 1.7 to 2.7GHz. Evidence of this phenomenon can be found in Fig. 11, where the current distribution on the LB CE created by the HB antenna is displayed for different frequencies. It is seen that the currents on the HB antenna are weaker at 2GHz while the currents on the LB CE are stronger, which suggests a high level of coupling. However, the current induced on the LB CE are prevented from flowing to the LB feed by the LB MN and the port-to-port isolation is kept high in this manner. From the behavior of the currents at 2.3GHz, we see that the HB antenna is strongly excited whereas the coupling to the LB CE is relatively weak.

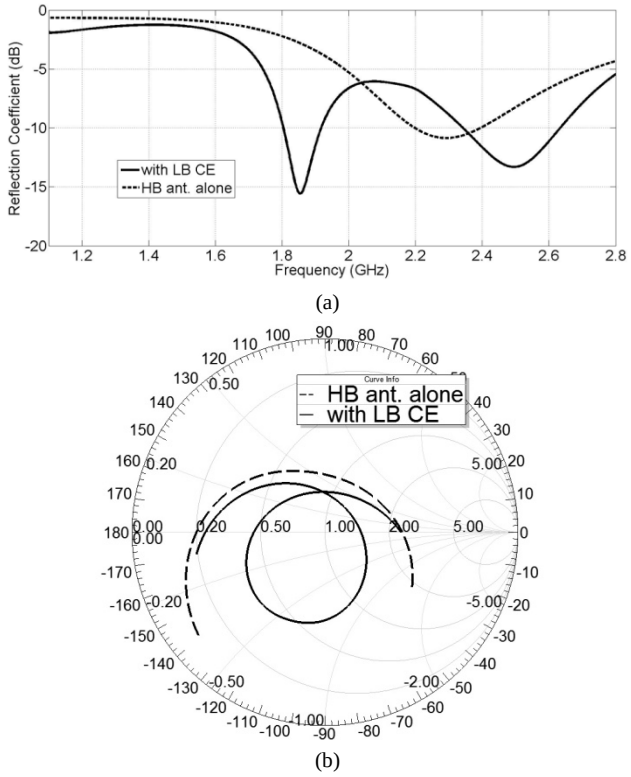

Fig. 10. Simulated input impedance of the HB antenna alone and with the LB CE (a) magnitude of the reflection coefficients, (b) input impedance on Smith Chart

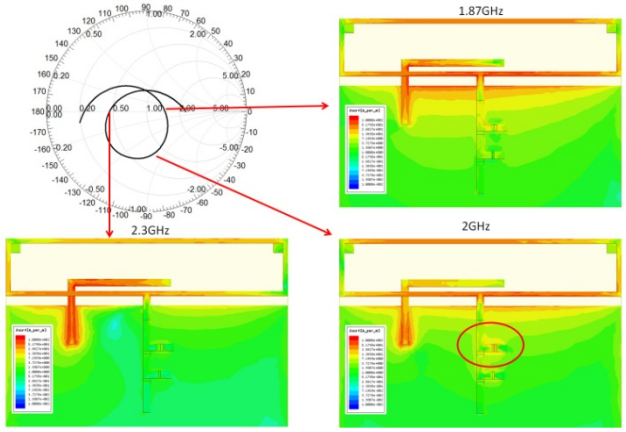

Fig. 11. Current distributions on the LB CE when the HB antenna port is excited at various frequencies: 1.87 GHz, 2 GHz, 2.3 GHz

C. *Measurement Results*

The optimized antenna shown in Fig. 6 was fabricated on an FR4 substrate (Fig. 12). Fig. 9 and Fig. 13 show that, there is a fair agreement between the simulated and measured S-parameters. The target bands are indeed covered with a reflection coefficient below -6dB.

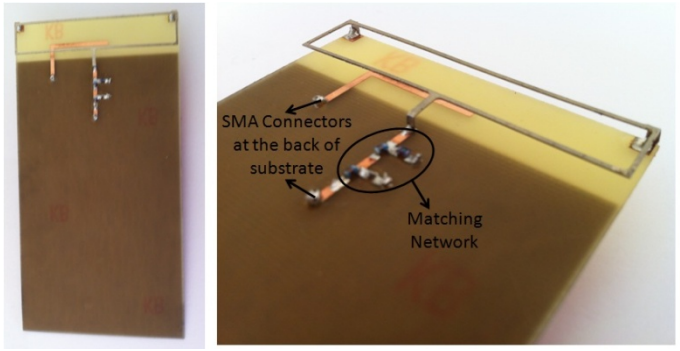

Fig. 12. Pictures of the manufactured antenna prototype

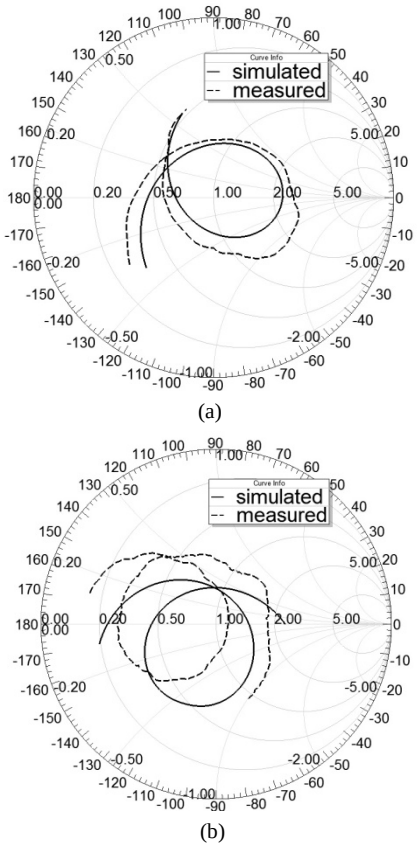

Fig. 13. Simulated and measured input impedance of the optimized antenna presented in Fig. 6 and 12. (a) LB port between 700-960MHz, (b) HB port between 1.7-2.7GHz

The total efficiency and the 3D gain patterns have also been measured in a Satimo Starlab Station. The total efficiency of the proposed antenna in LB and HB are presented in Fig. 14(the HB port is loaded with 50Ω when the LB efficiency is measured and vice versa). The measured total efficiency (including mismatch and component losses) in LB varies between -6dB and -2dB (generally higher than -4dB) and between -4dB and -1dB in HB. Fig. 15 shows a fair

agreement between the simulated and measured 3D gain patterns. In LB, a dipole-type radiation is observed (as expected) since the main radiator is the ground plane. In either the LB or HB, no wide-angle deep nulls are seen in the radiation patterns which is an important aspect for mobile phone communications where the base-station orientation is never known in advance.

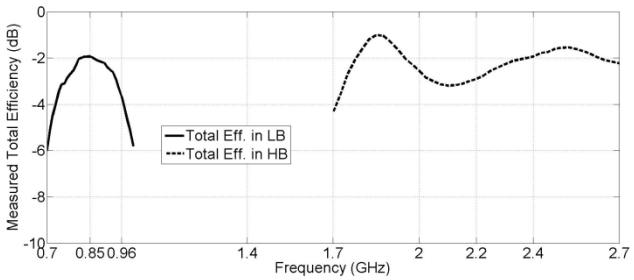

Fig. 14. Measured total efficiency of the proposed antenna

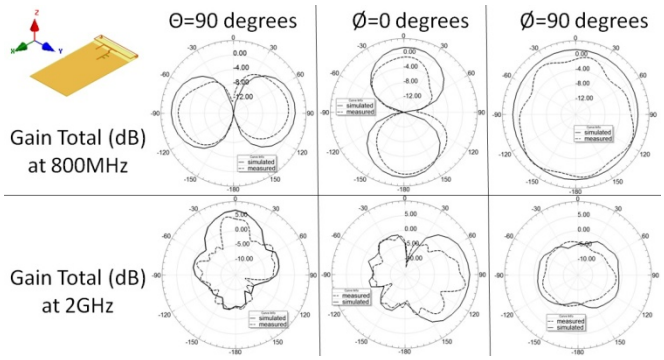

Fig. 15 Simulated and Measured total Gain radiation pattern in dB for different cut planes of the proposed antenna presented in Fig. 6

III. Printed Hollow Coupling Element Antenna

A. *Antenna Design*

The approach presented in Section II for a 3mm height 3D hollow CE was then applied to design an antenna-structure, which is totally printed on the FR4 substrate. Ease of manufacturing and low cost are the main advantages of this technological approach (Fig. 16). The main difference between the previous antenna structure and the present one is the location of the printed HB antenna on the FR4 substrate. Since it was not possible to integrate the HB antenna inside the printed hollow CE, we placed it at the left side of the PCB, where the E-field was simulated to be the weakest. The PCB and ground plane dimensions were set to be the same as the previous antenna structure. The dimensions of the optimized hollow CE were optimized to be 59×4mm^2 with a strip width of 1mm. Another major difference is also the values of the components of the MN. Moreover, a two-component MN was found to be necessary at the HB antenna port.

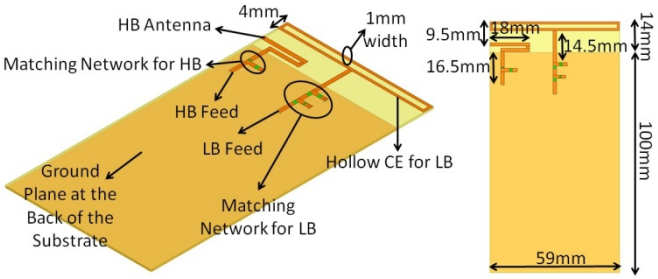

Fig. 16. 3D and top view of the optimized printed hollow CE antenna

The effect of hollowing out the printed CE, instead of using a printed plain CE, was investigated. The comparison of the Bandwidth Potential of a printed plain CE and a printed hollow CE with identical outer dimensions is shown in Fig. 17. In this case, making the printed CE hollow helps to cover an extra 25MHz matching bandwidth around the center frequency of the LB with a two-element MN (-6dB reflection coefficient). This is mainly due to the ring-shape of the hollow CE, which provides an inductive effect on its input impedance.

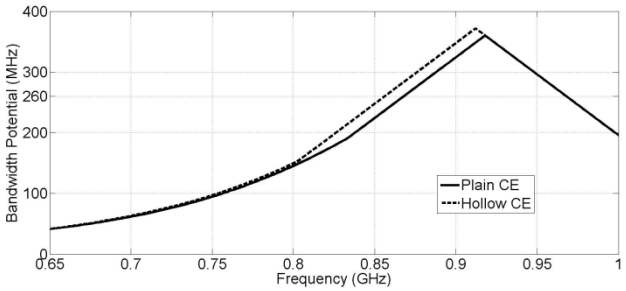

Fig. 17. Bandwidth Potential of a plain and hollow CE in 2D printed configuration (outer dimensions are 59×4mm^2)

The MNs for both the LB and HB antenna ports were designed with Optenni Lab software (Fig. 18). For the optimization of the LB antenna, it was desired to have a band-pass behavior between 700 and 960MHz and a band-stop effect from 1.7 to 2.7GHz. Complementary goals were assigned for the HB MN to achieve even higher LB isolation than the 9 dBs obtained with the previous 3D antenna. The component values were then fine-tuned with the full-wave electromagnetic simulator by taking the linking transmission lines and vias into account.

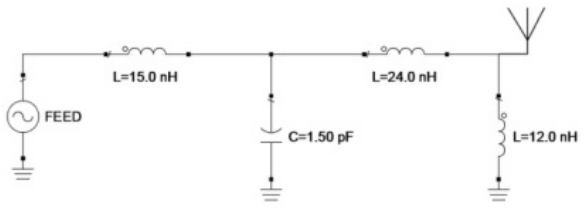

(a)

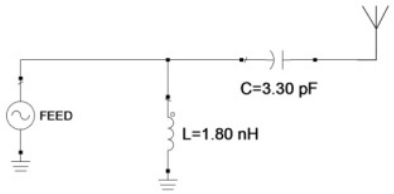

(b)

Fig. 18. MN topologies and component values for (a) LB and (b) HB ports

The simulated input impedance of the printed CE alone can be seen in Fig. 19 with and without the MN. The simulated S-parameters for the entire structure, including the HB antenna, are presented in Fig. 20. The target frequency bands are covered with a reflection coefficient below -6dB except for an overshoot between 700 and 720MHz. The achieved isolation level is greater than 23dB in both bands, which is a consequence of both the antenna placement and the band-stop behavior of the two MN's.

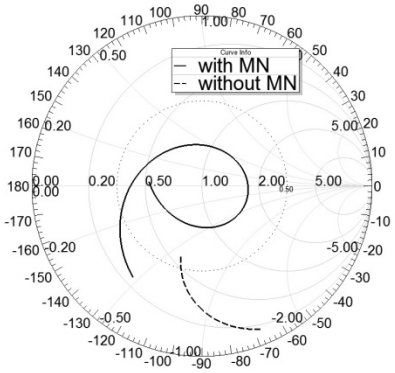

Fig. 19. Simulated input impedance of the printed CE alone with and without MN

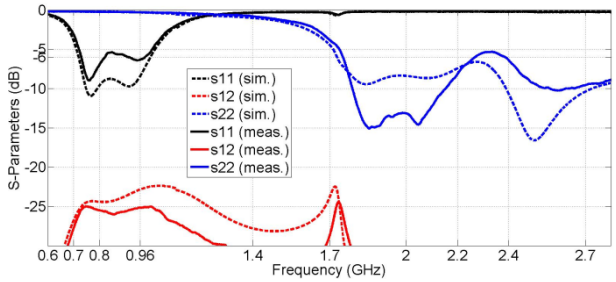

Fig. 20 Simulated and measured S-parameters of the printed antenna structure presented in Fig. 16

To explain the wideband behavior of the HB antenna, we plotted its input impedances alone, as well as associated with the LB CE (Fig. 21). Additional resonances are created from the coupling between this HB antenna and the LB CE. For instance, the HB antenna is strongly excited at 1.8GHz (Fig. 22) whereas the excitation is lower with a larger coupling with the LB CE at 2.5GHz. Although there exists some coupling between both antennas at different frequencies, a high isolation is still maintained with the help of the band-stop characteristics of the MNs.

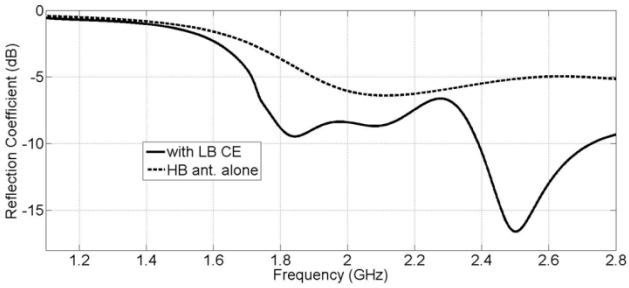

(a)

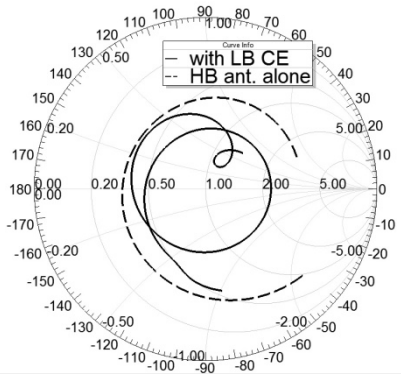

(b)

Fig. 21. Simulated input impedance of the HB antenna alone and with the LB CE (a) magnitude of the reflection coefficients, (b) input impedance on Smith Chart

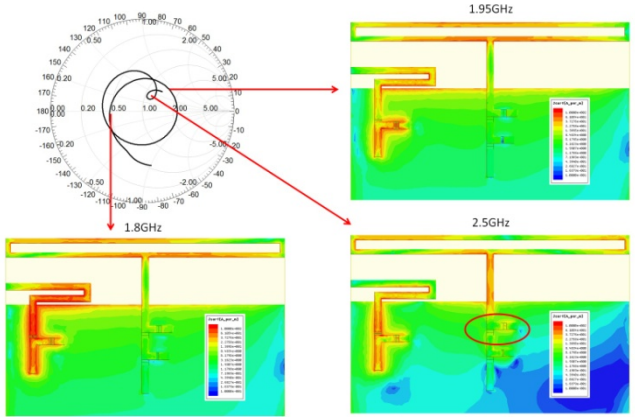

Fig. 22. Current distribution on the LB CE when the HB antenna port is excited at various frequencies: 1.8 GHz, 1.95 GHz, 2.5 GHz

B. Measurement Results

The printed antenna structure has been fabricated on an FR4 substrate (Fig. 23). The comparison of the simulated and measured S-parameters are shown in Fig. 20 and on Smith Chart in Fig. 24. There is a fair agreement between the simulated and measured results. The proposed printed antenna can cover the target bands with a measured reflection coefficient below -6dB except for the frequency interval of 700-720MHz and also with a small overshoot up to -5.5dB around 850MHz.

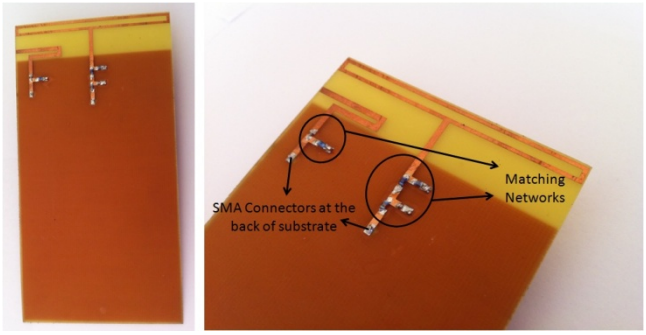

Fig. 23. Manufactured printed antenna prototype presented in Fig. 16

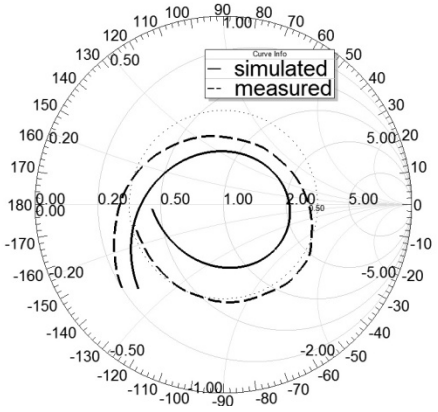

(a)

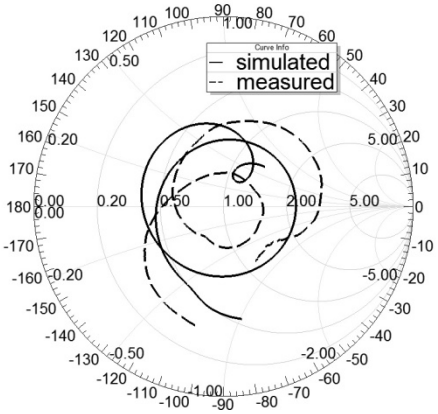

(b)

Fig. 24. Simulated and measured input impedance of the optimized printed antenna presented in Fig. 16 and 23 (a) LB port 700-960MHz, (b) HB port 1.7-2.7GHz

The total efficiency was measured to vary from -5dB to -1.5dB in the LB and from -4dB to -1.2dB in the HB. The simulated and measured 3D gain radiation patterns are also in good agreement, as seen from Fig. 26.

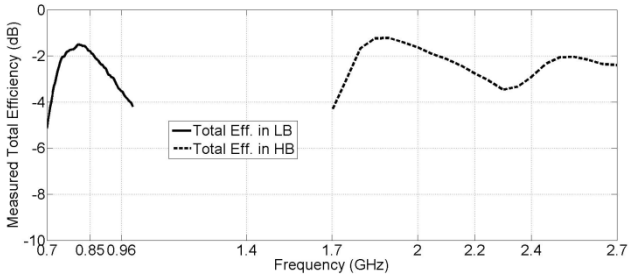

Fig. 25. Measured total efficiency of the printed antenna

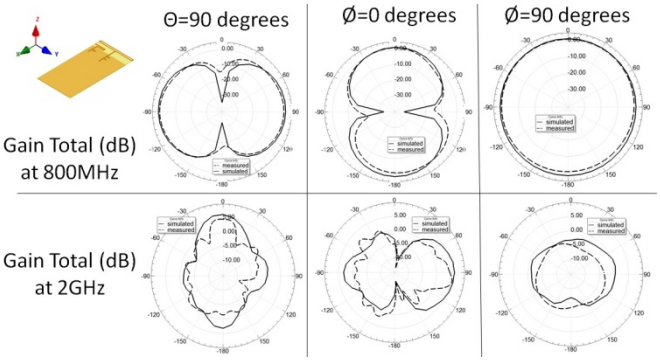

Fig. 26. Simulated and Measured 3D Gain patterns (Total in dB) of the antenna from Fig. 23 in different cut planes

IV. Effect of the User's Hand

To see the effect of the user's hand on the two proposed antenna topologies, both S-parameter and total efficiency measurements were carried out with a CTIA hand phantom. The measurement setups for the S-parameter and total efficiency measurements are presented in Fig. 27.

(a) (b)

Fig. 27. Pictures of the measurements with CTIA hand phantom (a) S-parameter configuration, (b) total efficiency configuration

Two holding configurations were tested for the S-parameter and efficiency measurements as the "bottom configuration", depicted in Fig. 27, where the antenna is located at the bottom of the PCB facing the palm and the "top configuration" where the antenna is located at the top of the PCB facing the index finger.

For the first antenna structure presented in Section II, the S-parameter and total efficiency measurements can be seen in Fig. 28 and Fig. 29. The S-parameter detuning, due to the presence of the hand is more effective in the LB, observed as a resonance shift towards the lower frequencies when compared to the free space (FS) case. The measured total efficiency in the LB is found to be around -6dB for "top configuration" and -7.5dB for "bottom configuration". The efficiency decrease is higher in this "bottom configuration" since the antenna directly faces the lossy palm. In "top configuration", only the index finger is in the vicinity of the antenna, hence the efficiency decrease is lower.

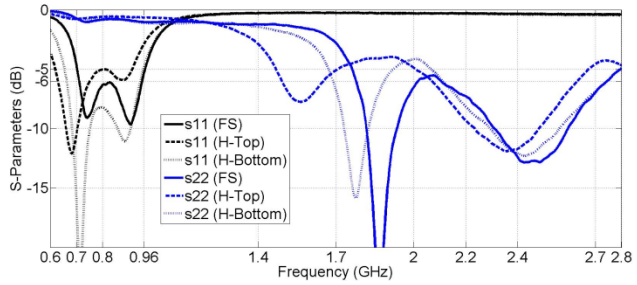

Fig. 28. Measured S-parameters for the 3D antenna with and without the hand of the user (and also free space)

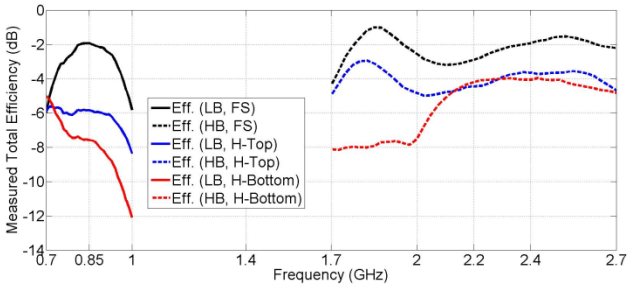

Fig. 29. Measured total efficiency for the 3D antenna with and without the hand (and also free space)

Measurement results for the printed antenna are presented in Fig. 30 and Fig. 31. The same frequency shift toward the low frequencies can be observed. The LB total efficiency is found to be around -6dB in "top configuration" and -8.5dB in "bottom configuration". The efficiency decrease is again higher for the "bottom configuration", as expected.

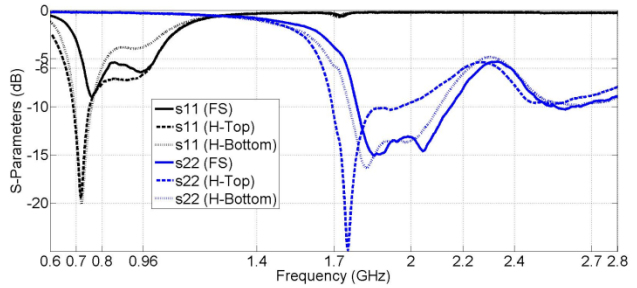

Fig. 30. Measured s-parameters for the printed antenna with and without the hand of the user (and also free space)

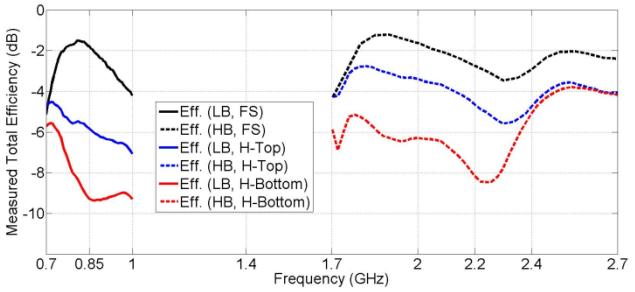

Fig. 31. Measured total efficiency for the printed antenna with and without the hand of the user (and also free space)

V. Conclusions

A novel approach for antenna designs targeting 700-960MHz and 1.7-2.7GHz operation in handheld terminals has been presented in this paper. This approach consists of using a CE which is made hollow by removing the metal inside for 700-960MHz coverage with negligible performance trade-off. In this way, the space inside and underneath the CE is made available for the integration of another antenna to cover the 1.7-2.7GHz band, with a separate feed. To achieve high port-to-port isolation, the HB antenna is placed in a weak E-field region and also the MNs are optimized to ensure band-stop behavior in the operating frequency of the neighbor antenna. Using this methodology, two antenna structures were designed and fabricated, one with a 3mm height CE and the other with a printed CE. For both prototypes, it was shown that the antennas can cover the target bands with -6dB reflection coefficient. The total efficiency measurements in free-space were also carried out in a Satimo Starlab station, showing efficiencies up to -2dB and -1.5dB in the LB and HB, respectively. Finally, to investigate the effect of the user's hand on the S-parameter and total efficiency, measurements were performed with a CTIA hand phantom showing a reasonable detuning and acceptable total efficiency which demonstrates the interest for our novel concepts. It is wortwhile emphasizing that the second fully-printed structure has a very simple shape and less sensitivity to manufacturing tolerances which is definitely very desirable for mass production at low cost.

Acknowledgments

CIMPACA design platform is acknowledged for support.

References

[1] 3GPP Specification Detail, Available at: http://www.3gpp.org/ftp/Specs/html-info/36101.htm

[2] P. Vainikainen, J. Ollikainen, O. Kivekäs, and I. Kelander, Patent FI114260, Modular coupling structure for a radio device and a portable radio device, Finland, Appl. 20002529, 17.11.2000, (15.09.2004), 22 p.

[3] P. Vainikainen, J. Ollikainen, O. Kivekas, I. Kelander, "Performance Analysis of Small Antennas Mounted on Mobile Handsets," Proceedings of the COST 259 Final Workshop-Mobile and Human Body Interaction, 2000, p. 8.

[4] P. Vainikainen, J. Ollikainen, O. Kivekas, I. Kelander, "Resonator-based analysis of the combination of mobile handset antenna and chassis," IEEE Transactions on Antennas and Propagation, vol.50, no. 10, pp.1433-1444, October 2002.

[5] J. Villanen, J. Ollikainen, O. Kivekas, P. Vainikainen, "Coupling element based mobile terminal antenna structures," IEEE Transactions on Antennas and Propagation, vol.54, no.7, pp. 2142,2153, July 2006.

[6] J. Holopainen, R. Valkonen, O. Kivekas, J. Ilvonen, P. Vainikainen, "Broadband Equivalent Circuit Model for Capacitive Coupling Element–Based Mobile Terminal Antenna," IEEE Antennas and Wireless Propagation Letters, vol. 9, pp. 716-719, 2010.

[7] J. Villanen, C. Icheln, P. Vainikainen, "A coupling element-based quad-band antenna structure for mobile terminals," Microwave and Optical Technology Letters, vol. 49, no. 6, June 2007, pp. 1277–1282.

[8] A. Andujar, J. Anguera, C. Puente, "Ground Plane Boosters as a Compact Antenna Technology for Wireless Handheld Devices," IEEE Transactions on Antennas and Propagation, vol. 59, no. 5, pp. 1668-1677, May 2011.

[9] W.L. Schroeder, P. Schmitz, C. Thome, "Miniaturization of mobile phone antennas by utilization of chassis mode resonances", German Microwave Conference, 2006.

[10] D. Manteuffel, M. Arnold, "Considerations on configurable multi-standard antennas for mobile terminals realized in LTCC technology," 3rd European Conference on Antennas and Propagation 2009 (EuCAP 2009), pp. 2541-2545, 23-27th March 2009.

[11] R. Valkonen, J. Ilvonen, P. Vainikainen, "Naturally non-selective handset antennas with good robustness against impedance mistuning," 6th European Conference on Antennas and Propagation 2012 (EUCAP 2012), pp.796-800, 26-30th March 2012.

[12] R. Valkonen, J. Ilvonen, C. Icheln, P. Vainikainen, "Inherently non-resonant multi-band mobile terminal antenna," IET Electronics Letters, vol. 49, no. 1, pp. 11-13, 3rd January 2013.

[13] F.-H. Chu, K.-L. Wong, "Internal coupled-fed loop antenna integrated with notched ground plane for wireless wide area network operation in the mobile handset," Microwave and Optical Technology Letters, vol. 54, no. 3, pp. 599–605, March 2012.

[14] C.-W. Yang, Y.-B. Jung, C.-W. Jung, "Octaband Internal Antenna for 4G Mobile Handset," IEEE Antennas and Wireless Propagation Letters, vol.10, pp.817-819, 2011.

[15] W-S. Chen, B-Y. Lee, Y-T. Liu, "A printed coupled-fed loop antenna with two chip inductors for the 4G mobile applications," Microwave and Optical Technology Letters, vol. 54, no. 9, pp. 2157–2163, September 2012.

[16] C.-W. Chiu, C.-H. Chang, Y.-J. Chi, "A meandered loop antenna for LTE/WWAN operations in a smart phone," Progress In Electromagnetics Research C, vol. 16, pp. 147-160, 2010.

[17] S-C. Chen, K-L. Wong, "Wideband monopole antenna coupled with a chip-inductor-loaded shorted strip for LTE/WWAN mobile handset," Microwave and Optical Technology Letters, vol. 53, no. 6, pp. 1293–1298, June 2011.

[18] S-C. Chen, K-L. Wong, "Small-size 11-band LTE/WWAN/WLAN internal mobile phone antenna," Microwave and Optical Technology Letters, vol. 52, no. 11, pp. 2603–2608, November 2010.

[19] F-H. Chu, K-L. Wong, "On-board small-size printed LTE/WWAN mobile handset antenna closely integrated with system ground plane," Microwave and Optical Technology Letters, vol. 53, no. 6, pp. 1336–1343, June 2011.

[20] C-T. Lee, K-L. Wong, "Planar Monopole With a Coupling Feed and an Inductive Shorting Strip for LTE/GSM/UMTS Operation in the Mobile Phone," IEEE Transactions on Antennas and Propagation, vol. 58, no. 7, pp. 2479-2483, July 2010.

[21] K-L. Wong, M-F. Tu, T-Y. Wu, W-Y. Li, "Small-size coupled-fed printed PIFA for internal eight-band LTE/GSM/UMTS mobile phone antenna," Microwave and Optical Technology Letters, vol. 52, no. 9, pp. 2123–2128, September 2010.

[22] K-L. Wong, W-Y. Chen, C-Y. Wu, W-Y. Li, "Small-size internal eight-band LTE/WWAN mobile phone antenna with internal distributed LC matching circuit," Microwave and Optical Technology Letters, vol. 52, no. 10, pp. 2244–2250, October 2010.

[23] A. Cihangir, F. Sonnerat, F. Ferrero, C. Luxey, R. Pilard, F. Gianesello, G. Jacquemod, "Design of traditional and a novel space-efficient antenna-coupling elements for lower LTE/GSM mobile phones," Loughborough Antennas and Propagation Conference 2012 (LAPC 2012), pp. 1-4, 12-13th November 2012.

[24] A. Cihangir, F. Ferrero, C. Luxey, G. Jacquemod, "A space-efficient coupling element antenna for WWAN applications," International Workshop on Antenna and Technology 2013 (iWAT2013), pp. 55-58, 4-6th March 2013.

[25] ANSYS HFSS, Available at: http://www.ansys.com/products/hf/hfss/

[26] Optenni Lab, Available at: http://www.optenni.com/optenni-lab/

Aykut Cihangir was born in Ankara, Turkey in 1985. He received his Bachelor's degree from Electrical and Electronics Engineering Department of Middle East Technical University (METU) in Ankara in 2007. From 2007 to 2011, he worked in Turkish Aerospace Industry (TAI) as a Communication Systems Design Engineer in Unmanned Aerial Vehicle projects. At the same period until 2010, he completed his Master's Degree study in METU about radiation characteristics of tapered slot antennas in millimeter-wave frequencies. From 2011 to 2014, he did his PhD study in the Laboratory of Electronics, Antennas and Telecommunications in University of Nice-Sophia Antipolis (UNSA) in France on electrically small antennas and matching networks for 4G mobile terminals and obtained his PhD degree in 2014. He is currently working as a Post-Doc researcher in UNSA in EpOC team. His current research interests include electrically small antennas, matching networks and mobile terminal antennas. He was awarded with the third place in the best student paper contest in LAPC 2013 international conference.

Fabien FERRERO was born in Nice, France in 1980. He finalized his EPU engineer degree in electronics and his Master Propagation, Télédétection and Télécommunications in EDSTIC of Sophia Antipolis in 2003. He received the Ph.D. degree in electrical engineering in 2007 from the University of Nice-Sophia Antipolis. From 2008 to 2009, he worked for IMRA Europe (Aisin Seiki research center) as a research engineer and developed automotive antennas. He is currently an Associate Professor at the Polytechnic school of the University of Nice Sophia-Antipolis. He is co-director of the joint lab between University of Nice and Orange, the CREMANT (Centre de Recherche Mutualisé sur les Antennes). His studies concerned design and measurement of millimetric antennas, miniature and reconfigurable antennas.

Gilles Jacquemod graduated from ICPI (CPE) Lyon, and received MSc degree (DEA) in microelectronics from Ecole Centrale Lyon in 1986. He received the Ph.D. degree in integrated electronics from INSA Lyon, in 1989. From 1990 to 2000, he worked at LEOM, Ecole Centrale Lyon, as an Associate Professor, on analog integrated circuit design and behavioral modeling of mixed domain systems. He was also involved in the application of signal processing and communication systems. In 2000, he joined the LEAT laboratory and the Ecole Polytechnique of Nice-Sophia Antipolis University as full professor. Since 2010, he is with EpOC research team (URE UNS 006). His primary research interests include analog integrated circuit design and behavioral modeling of mixed domain systems. He is also involved in RF design applied to wireless communication. He is director of the CNFM PACA pole. He is President of the CIM-PACA Design Platform. He was advisor more than 25 PhD students. He is author and co-author of more than 200 journal and conference papers, and holds 2 patents.

Patrice Brachat was born in Gourdon (France) in 1955. He received a degree in telecommunications and electricity from Ecole Nationale Supérieure des Télécommunications (ENST), Paris, in 1978 and a Ph.D. degree from Université Paul sabatier Toulouse in 1980 and the HdR (Habilitation à diriger les Recherches) degree from Université de Nice Sophia Antipolis in 1998. In 1981 he joined the antenna departement of France Telecom Research and Development and since 1992 he has been in charge of an Antenna Research Group in the La Turbie Orange Lab. Since 1992 he has also held scientific appointments at university of Nice Sophia Antipolis (France). Since 2008 and until 2014 he has been co-head of the CREMANT, the antenna joint research center between the Orange Labs, the Nice University and the CNRS (National Scientific Research Center) His professional interests include the areas of antenna design, small antennas, computational electromagnetics, electromagnetic modeling and simulation. He has published over 80 papers in journals or conferences, and holds 14 patents in these fields. In 1982 he participated in the creation of JINA conference in NICE (Journées internationales de Nice sur les Antennes). Since 1982 he has been a member of the JINA steering committee, in 1998 he was in charge of scientific secretariat and since 2000 he has been the vice chairman of this conference. In 2006 he contributed to the birth of the EuCAP conference and was local chairman of the successful EuCAP06 edition in Nice. Since 2006 he has been a member of the EuCAP Technical Committee and senior member IEEE.

Cyril Luxey was born in Nice, France in 1971. He received the DEA (Master degree 1996) and the Ph.D. degree in electrical engineering (1999), both with honors (Summa Cum Laude), from the University Nice-Sophia Antipolis, France. During his thesis, he worked on several antenna-solutions for

automotive applications like printed leaky-wave antennas, quasi-optical mixers and retrodirective transponders. From 2000 to 2002, he was with Alcatel, Mobile Phone Division, Colombes, France, where he was involved in the design and integration of internal antennas for commercial mobile phones. In 2003, he was recruited as an Associate Professor at the Polytechnic school of the University Nice Sophia-Antipolis. Since 2009, he is a Full Professor at the IUT Réseaux et Télécoms in Sophia-Antipolis where he is the head of a technical bachelor degree. He is doing his research in the EpOC team and he is co-head of this team. In October 2010, he has been appointed as a Junior Member of the Institut Universitaire de France (IUF) institution for five years. His current research interests include the design and measurement of Millimeter-wave antennas, electrically small antennas (theoretical limits and Wheeler cap techniques), antennas in-package, LTCC modules for 60 and 120 GHz applications, multi-antenna systems for diversity and MIMO techniques, mm-wave front end until 140 GHz. Cyril Luxey is an IEEE Senior Member. He is an associate editor for *IEEE Antennas and Wireless Propagation Letters*, a reviewer for the *IEEE Transactions on Antennas and Propagation*, the *IEEE Antennas and Wireless Propagation Letters*, the *IEEE Transactions on Microwave Theory and Techniques*, the *IEEE Microwave and Wireless Conference Letters*, the *IET Electronics Letters*, the *IET Microwave Antennas and Propagation* journals and several European and US conferences in the field of microwave, microelectronics and antennas. Cyril Luxey and his students received the *H.W. Wheeler Award* of the IEEE Antennas and Propagation Society for the best application paper of the year 2006. Cyril Luxey is also the co-recipient of the *Jack Kilby Award 2013 of the ISSCC conference*. He is the co-recipient of the best paper of the EUCAP2007 conference. He is also the co-recipient of the best-paper award of the International Workshop on Antenna Technology (iWAT2009). Cyril Luxey is the co-recipient of the best paper award at LAPC 2012 and the co-recipient of the best student paper at LAPC 2013 (3rd place). Cyril Luxey has authored or co-authored more than 250 papers in refereed journals, in international and national conferences and as book chapters. He has given more than 15 invited talks. Cyril Luxey has been the general co-chair of the Loughborough Antennas and Propagation Conference 2011, the award and grant chair of EuCAP 2012 and the invited paper co-chair of EuCAP 2013. He is a lecturer in the European School of Antennas for the "Industrial Antennas" course held at IMST. He is also the one of the French Delegate of the COST IC1102 action VISTA (Versatile, Integrated, and Signal-aware Technologies for Antennas) within the ICT Domain.